Available online at www.sciencedirect.com
ScienceDirect
Polymer 48 (2007) 7404–7413
polymer
www.elsevier.com/locate/polymer

Double yielding in PA6/TPV–MAH blends: Effect of dispersed phase with different content, modulus

Xue-Gang Tang [a], Wei Yang [a,b,*], Gui-Fang Shan [a], Ming-bo Yang **, Bang-hu Xie [a], Qiang Fu [a]

[a] College of Polymer Science and Engineering, Sichuan University, State Key Laboratory of Polymer Materials Engineering, Chengdu, 610065 Sichuan, China
[b] The Key Laboratory of Polymer Processing Engineering, Ministry of Education, South China University of Technology, China

Received 6 June 2007; received in revised form 25 September 2007; accepted 28 September 2007
Available online 22 October 2007

Abstract

In this study, we have investigated the effect of thermoplastic vulcanizates (TPV) content and characteristic on the double yielding of injection molded polyamide 6 (PA6)/TPV blends uniaxially tensile deformed at room temperature. The results indicated that the TPV content and characteristic showed a marked effect on the double yielding phenomenon. The morphological observation by scanning electron microscope (SEM) showed that the injection molded PA6/TPV blends displayed a typical skin–core structure with highly oriented TPV particles in the skin and sub-skin layers, and spherical TPV particles in the core layer. Combining the microscopic morphology and stress–strain behavior, a possible model for description of the double yielding behavior of the PA6/TPV blends was proposed. The first yield point might be caused by the deformation of the matrix and the dispersed phase in the skin and sub-skin layers, while the second yield point is correlated with the deformation of the dispersed phase in the core layer.

Keywords: Double yielding; PA6/TPV–MAH blend; Deformation

1. Introduction

Polymer blending is an economical route to get new polymer materials at low cost and to combine the performances of the corresponding pure polymers [1–5]. Blending of different polymers which are often immiscible with each other, results in a two-phase morphology with the minor phase in the form of spherical droplets, platelets, or fibers [6,7]. Multicomponent blends based on polyamide 6 (PA6) have gained tremendous attention in industrial applications owing to the combination of excellent mechanical properties and processability [8,9]. The compatibilizer introduced either as a third component or developed in situ through reactive processing at a reduced concentration is necessary to reduce the interfacial tension and the dispersed phase size, to improve the interfacial adhesion and subsequently to improve the mechanical properties, leading to a more stable morphology normally. In situ compatibilization is a good way to improve the mechanical properties of PA6 blends [10–12].

The deformation behavior and ultimate mechanical properties are very important characteristics of polymers and polymer blends for engineering applications, especially, the yield behavior, because the yield strength represents the limit of allowable (tensile) stress of a material [13] and understanding the yielding process is very important to give a clear-cut description of the complete deformation process.

Conventionally, the yield point in polymers is regarded as the point where the stress–strain curve shows a local maximum [14,15]. This point is generally accepted to be related to the onset of necking, where the strain hardening of the necked material is not sufficient to counteract the reduction

* Corresponding author. College of Polymer Science and Engineering, Sichuan University, State Key Laboratory of Polymer Materials Engineering, Chengdu, 610065 Sichuan, China. Fax: +86 28 8546 0130.
** Corresponding author.
E-mail addresses: ysjsanjin@163.com (W. Yang), yangmb@scu.edu.cn (M.-b. Yang).

0032-3861/$ - see front matter © 2007 Elsevier Ltd. All rights reserved.
doi:10.1016/j.polymer.2007.09.052

in the cross-sectional area of the necked region [16]. However, the situation is more complicated since the appearance of double yielding phenomenon in low-density polyethylene (PE) of different branch contents, which was first reported by Popli and Mandelkern [17]. Since then, many studies have shown the existence of the double yielding phenomenon in several groups of polymers [15,18–24] and polymer blends [25–27]. Most studies of the double yielding behavior of polymers were focused on PE system, while this behavior was also found in PA6 system [28–32]. The occurrence of double yielding in PA6 films, carefully dried under vacuum, was first recognized by Hoashi et al. [33] without any comments. Previous work of our group on the double yielding of PA6 has found the mold temperature, moisture content, temperature and strain rate showed a marked effect on the double yielding phenomenon [28–32].

However, only a few studies have been reported on such a phenomenon in incompatible blends [25–27] and, no publication was found on the incompatible blend system with modified interface, to the best of the authors. Several mechanisms have been forwarded to explain the double yielding phenomenon in polymer blend system. For the blend of polycarbonate (PC) and high-density polyethylene (HDPE) [26], the first yield point was attributed to the yielding of PE at low strain and the second one the result of the yielding of the PC fibers at relatively higher strain. While for PA6/K resin blend [27], the first yield point occurs at the lower tensile stress was deemed to be caused by the deformation of the K resin matrix and the second yield point the permanent plastic deformation of the entanglement of PA6 chains and PB segments.

In the present paper, we report the existence of the double yielding phenomenon in a PA6/thermoplastic vulcanizates (TPV) blend, in situ compatiblized by maleic anhydride (MAH) to improve the interfacial characteristic, and the effect of the dispersed phase content and characteristic with different modulus considered. The mechanism for our system was discussed and a model to explain the double yielding phenomenon was put forward.

2. Experimental procedure

2.1. Materials

The polyamide 6 (PA6) resin used here was a commercial product of Xinhui Meida-DSM Nylon Slice Company Ltd., supplied in pellets, with the trademark M2800. The melt flow rate (MFR) of the resin is 4.09 g $(10\ \text{min})^{-1}$ at 275 °C, exerting a force of 325 g. The resin was dried for 12 h under vacuum at 100 °C before injection molding to avoid hydrolytic degradation. Isotactic polypropylene (iPP), with the trademark F401, was obtained from Lanzhou Petrochemical Company Ltd. Certain properties of the resin, provided by manufacturer, are as follows: MFR = 2.5 g/10 min according to ASTM D1238.79, density = 0.91 g cm^{-3} according to ASTM D1505-68, and a tacticity of 98%. EPDM (Nordel 4725p) was obtained from Dupont Dow Elastomers L.L.C., Wilmington, DE, U.S.A. It contains 70% ethylene and 4.9% ENB (ethylidene norbornene), with the Mooney viscosity ($ML_{2+10}^{125\ ^\circ C}$) and $\overline{M}_w$ of 25 and 135,000, respectively. Dicumyl peroxide (DCP) was purchased from Shenyang Xinxi Reagent Firm (molecular weight = 270.37). Maleic anhydride (MAH) was obtained from Chengdu Kelong Chemical Reagent Firm (molecular weight = 98.06).

2.2. Sample preparation

2.2.1. Preparation of TPV-g-MAH

The preparation of TPV-*g*-MAH is referred to reports [34–40] and detailed procedure is as follows. The melt reactive blending process for preparing TPV-*g*-MAH samples composed of 30/70, 50/50, 70/30, PP/EPDM w:w, was carried out in an SHJ-20 co-rotating twin-screw extruder with a screw diameter of 25 mm and a length/diameter ratio of 23, and a temperature profile of 170, 180, 190, and 185 °C from the feeding zone to the die. The content of MAH was 2 wt% (the weight of polymer blends). The extrudate was then pelletized. For the sake of brevity, the different TPVs with different composition of PP/EPDM are denoted as TPV1 (30/70), TPV2 (50/50), TPV3 (70/30), respectively. TPVs with different graft yield were prepared by adding different MAH content with a PP/EPDM composition of 50/50. The MAH content is 0%, 0.5%, 1%, and 2%, the name of which was labeled as TPVa, TPVb, TPVc, and TPVd.

2.2.2. Preparation of PA6/TPV blends

After drying in vacuum at 100 °C over 12 h to remove the moisture, PA6 and TPV with predetermined proportion were melt blended in the extruder, with a temperature profile of 190, 230, 240, and 235 °C from the hopper to die. The extrudate was then pelletized. After drying to remove any moisture picked up during extrusion, the pellets were injection molded into dumb-bell tensile samples and impact samples on a PS40E5ASE precise injection-molding machine, with a temperature profile of 220, 230, 240, and 235 °C from the feeding zone to the nozzle. Both the injection pressure and the holding pressure were 37.4 MPa. The pure PA6 samples were directly injection molded under the same processing conditions.

2.3. Test

2.3.1. FTIR analysis

For FTIR analysis, several grams of the grafted TPV were first dissolved in xylene at its refluxing temperature. Then, the solution was precipitated by pouring into acetone, reposed for half an hour, followed by filtration using a funnel. The obtained precipitate was washed repeatedly with fresh acetone and dried in a vacuum oven at 60 °C to constant weight. The samples were then compression molded into thin films between aluminum sheets on a laboratory hot press at 200 °C under 10 MPa. FTIR spectra were determined on a Nicolet Magna-IR 560.

2.3.2. Determination of the grafting degree of MAH

The grafting degree of MAH in TPV is defined as the weight percentage of MAH in TPV-*g*-MAH graft copolymers.

It was determined by acid–alkali titration and the following procedures were adopted. One gram of purified sample was dissolved in 100 mL xylene at its refluxing temperature for half an hour. Then, the hot solution was titrated immediately with 0.1 mol/L KOH/C_2H_5OH, after adding four drops of 1% phenolphthalein in ethanol as indicator. Titration was stopped when the coloration lasted for 30 s. The sample was completely soluble at the refluxing temperature and did not precipitate during titration. Few drops of water were added to hydrolyze the anhydride group before titration. The equation to calculate the grafting degree of MAH in TPV-*g*-MAH can be expressed as follows:

$$\text{Grafting degree } (\%) = \frac{98.06 \times c \times (V - V_0)}{2 \times 1000 \times m} \times 100 \qquad (1)$$

where V (mL) and V_0 (mL) represent volumes of KOH/C_2H_5OH solution used for titrating grafted TPV and pure TPV, respectively; c (mol/L) is the molar concentration of KOH/C_2H_5OH solution; 98.06 (g/mol) is the molecular weight of MAH; m (g) is the weight of the grafted TPV; and the number 2 represents one anhydride group that would hydrolyze into two carboxylic acid groups after opening up of the anhydride ring. The data presented here were the average of three repeated analysis, and its relative mean deviation was less than 5%.

2.3.3. Tensile properties

The tensile measurements were performed at room temperature and the geometry of the test specimens, the number of test specimens, the test conditions, the procedure and calculations were according to ASTM D-638 except the selection of the cross-head speed, on an Instron 4032 universal test machine using the dumb-bell specimens. The cross-head speed of the apparatus was 20 mm/min, with the strain being determined on a 50 mm length zone in the middle part of the specimen by using an extensometer. The nominal strain rate is the ratio of the cross-head speed to the initial gauge length of the sample. Thus the strain rate was $0.67 \times 10^{-2}\ s^{-1}$.

2.3.4. SEM test

The phase morphology was observed with a JEOL JSM-5900LV scanning electron microscope (SEM). The samples were frozen in liquid nitrogen for 30 min, and then impact fractured for SEM analysis. The freshly fractured surface was gold sputtered before SEM observation. The accelerate voltage was 20 kV.

3. Results and discussion

3.1. Characteristics of different TPVs

Fig. 1 shows the moduli of the studied TPVs and PP, from which it can be seen that the modulus of three TPVs and PP is obviously different and the difference is quite large. The more PP content, the higher the modulus. Fig. 2 shows the stress–strain curves of the TPVs and PP, from which it can be seen

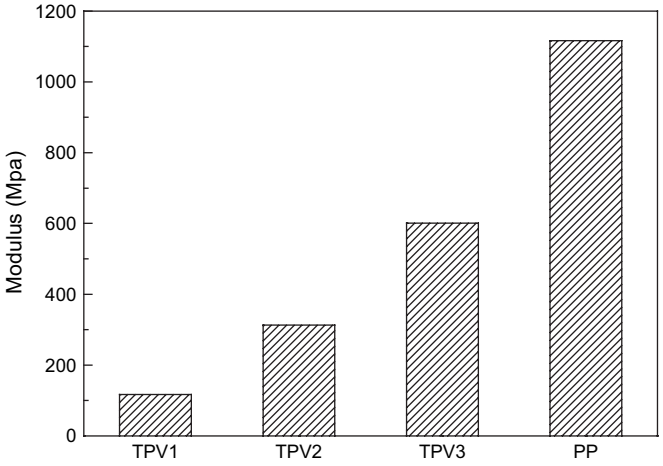

Fig. 1. The elastic moduli of different TPVs and PP.

that the stress–strain curve of TPV1 is similar to that of elastomers without yield point and TPV3 behaves as thermoplastic with distinct yield point, similarly to PP, while TPV2 is intervenient between TPV1 and TPV3. So the three TPVs show distinctly different characteristics, which is convenient for us to obtain general conclusions.

Fig. 3 shows the FTIR spectra of TPV2, from which it can be found that there is an absorbance peak at 1723 cm^{-1} in Fig. 3a and there are two peaks at 1723 and 1786 cm^{-1} in Fig. 3b. As we know, the absorbance of the carbonyl groups is from 1698 to 1856 cm^{-1} [41], so the absorbance peaks in 1723 and 1786 cm^{-1} are both the characteristic absorbance of carbonyl group. Comparing the two curves, there is an absorbance peak at 1786 cm^{-1} in Fig. 3b for the TPV with 2% MAH, which is the characteristic absorbance peak of acid anhydride, which confirms that MAH is grafted onto TPV successfully. The grafting degree (G) of TPV2 is 0.675%. The grafting degree (G) of TPVa, TPVb, TPVc and TPVd is 0%, 0.207%, 0.35%, and 0.675%, respectively.

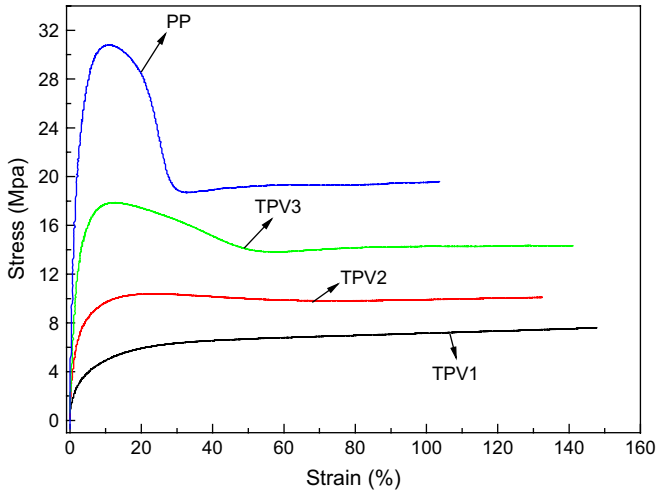

Fig. 2. Typical stress–strain curves of different TPVs and PP.

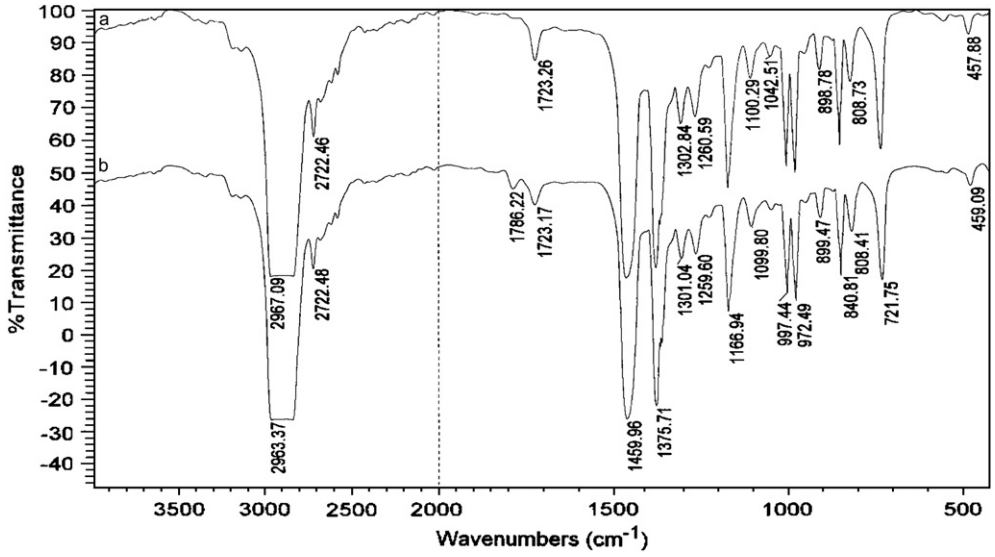

Fig. 3. FTIR spectrum of TPV-*g*-MAH: (a) without MAH; (b) with 2% (wt%) MAH.

3.2. The effect of dispersed phase content

Figs. 4–6 show the effect of different TPVs on the stress–strain curves of PA6/TPV system, with the respective TPV content increasing. It can be seen that there is double yielding phenomenon in all the PA6/TPV systems in our research and the TPV content shows a marked effect on the appearance of the stress–strain curve in the second yield point. The effect of TPV1 content on the stress–strain curves is shown in Fig. 4. It is evident that the stress of the first and the second yield point decreases with the increasing of TPV1 content, and the stress differences between the first and the second yield point decrease too, that is to say, the decreasing extent of the stress in the second yield point is smaller than that of the first yield point. At the same time, the strain of the first yield point does not change with the increasing of TPV1 content, while the strain of the second yield point increases, that is to say, the yield region between the first yield point and the second point becomes broader with the increasing of TPV1 content. Both Figs. 5 and 6 show the same trend. Because the three kinds of TPVs exhibit distinct characteristic and the variation is very distinct, it may be reasonable to state that double yielding may also can be observed in the range we studied.

3.3. The effect of different TPVs with the same content

Figs. 7–10 show the stress–strain curves of different characteristic TPVs with the same content (from 5% to 30%). It can be seen that the effect of TPV characteristic is not evident when the content is small (5% and 10%), while is significant when the content is large (20% and 30%), especially, on the stress of the first yield point. The higher the strength of TPV, the higher of the yield stress of both the first and second yield point.

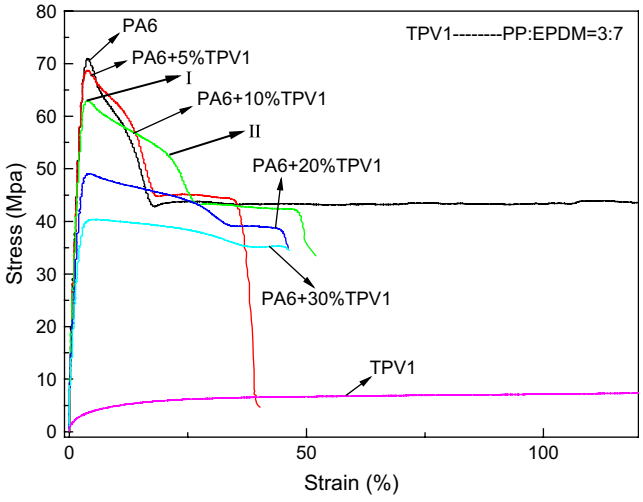

Fig. 4. Effect of TPV1 content on the double yielding phenomenon in PA6/TPV system (I is the first yield point and II is the second yield point).

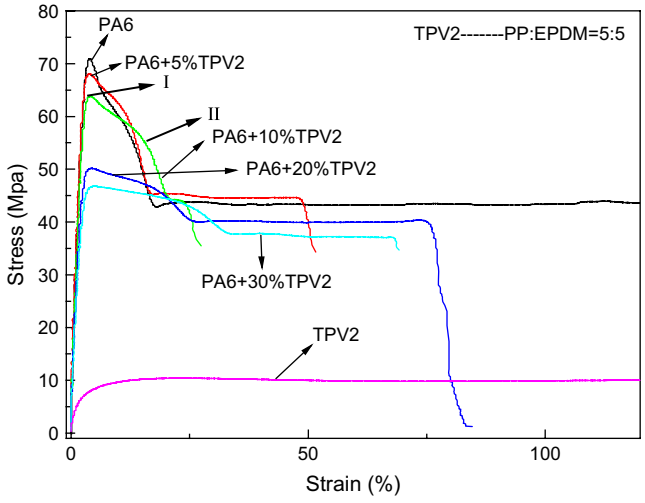

Fig. 5. Effect of TPV2 content on the double yielding phenomenon in PA6/TPV system (I is the first yield point and II is the second yield point).

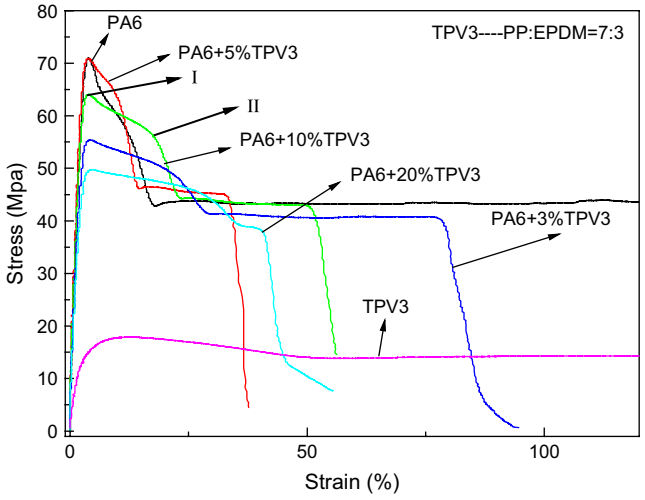

Fig. 6. Effect of TPV3 content on the double yielding phenomenon in PA6/TPV system (I is the first yield point and II is the second yield point).

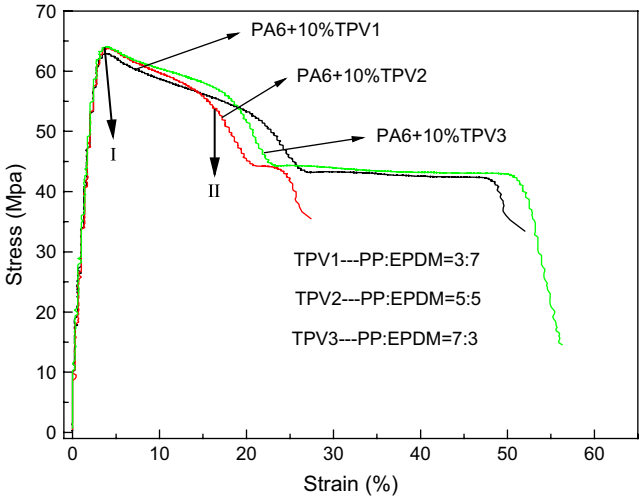

Fig. 8. Effect of different characteristic TPV with the content of 10% (wt%) (I is the first yield point and II is the second yield point).

3.4. The effect of interfacial interaction

In polymer blends, the interfacial interaction is an important influencing factor of the final mechanical properties. Here, the interfacial interaction was adjusted by controlling of the grafting degree of the dispersed phase, TPV. Fig. 11 shows the stress–strain curves of different characteristic TPVs with different grafting degree. It can be seen that the grafting degree of the dispersed phase shows a marked effect on the double yield behaviors shown in the stress–strain curves. When the grafting degree of the dispersed phase is 0%, the specimens fracture before the appearance of the second yield point. With the increasing grafting degree, that is, with the interfacial interaction of PA6 and the increasing dispersed phase, there is not much change in the first yield point, while the second yield point is quite different, that is, the strain of the second yield point decreases with the increasing interaction between PA6 and dispersed phase, although the stress shows little change.

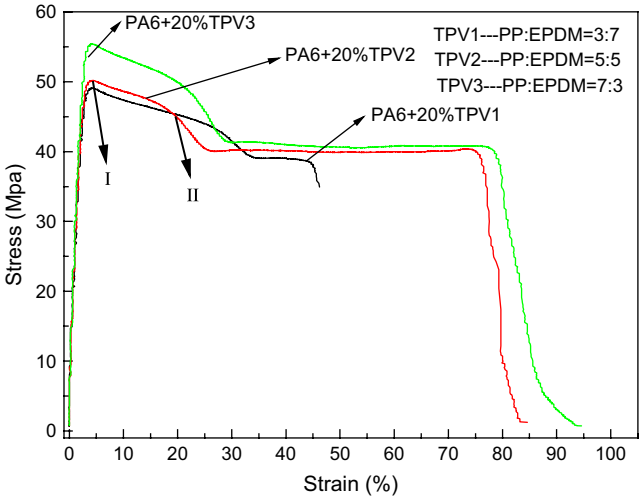

Fig. 9. Effect of different characteristic TPV with the content of 20% (wt%) (I is the first yield point and II is the second yield point).

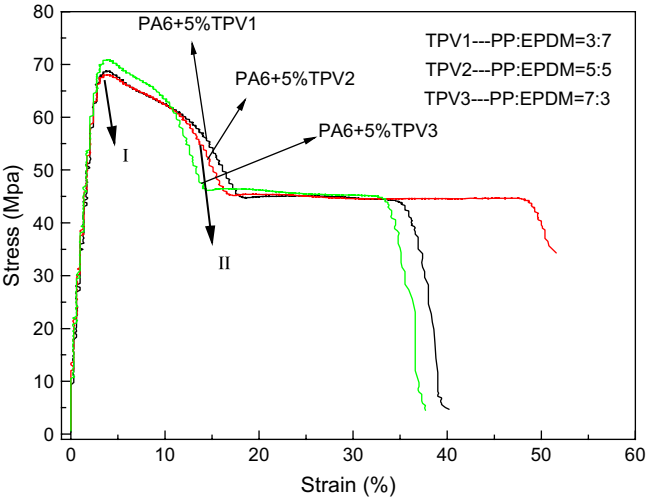

Fig. 7. Effect of different characteristic TPV with the content of 5% (wt%) (I is the first yield point and II is the second yield point).

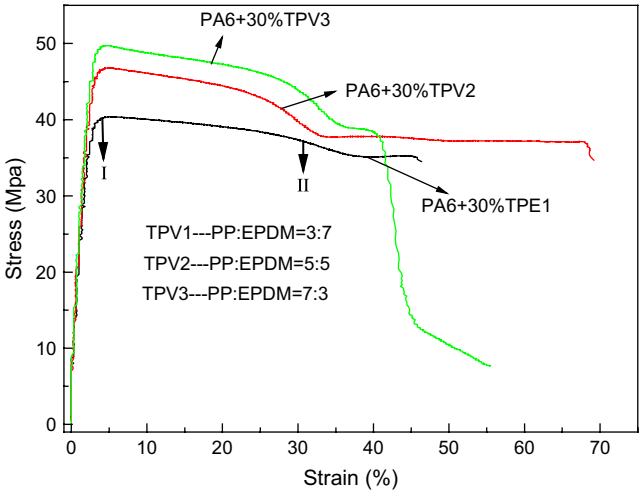

Fig. 10. Effect of different characteristic TPV with the content of 30% (wt%) (I is the first yield point and II is the second yield point).

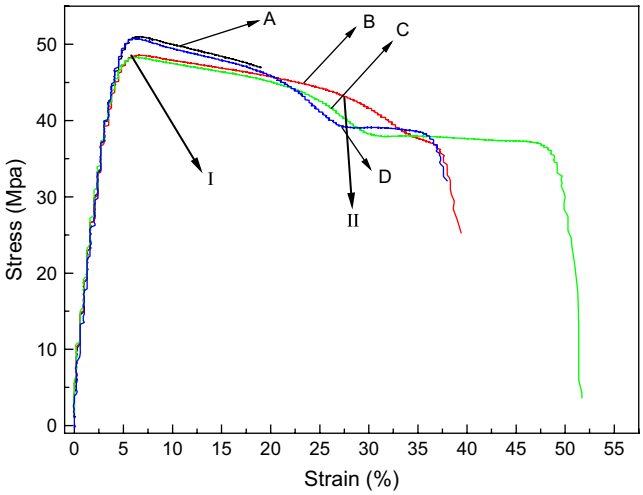

Fig. 11. The stress–strain curves of the blend of PA6 and TPV (the weight ratio is 8:2), the grafting degree of TPV is (A) 0%, (B) 0.207%, (C), 0.35%, and (D) 0.675%.

Detailed analysis of the results gives the following conclusions:

(1) The dispersed phase content shows a marked effect on the appearance of the stress–strain curve in the double yield point.
(2) The stress of the first yielding point decreases with the increasing of dispersed phase content, with the strain being constant (3.8%).
(3) The decreasing extent of the stress in the second yield point is smaller than that of the first yield point with increasing dispersed phase content, while the strain of the second yielding point increases.
(4) The characteristic of dispersed phase shows an effect on the double yielding phenomenon in PA6/TPV system, especially at relative high content of dispersed phase.
(5) The dispersed phase affects not only the second yield point, but also the first yield point.

3.5. SEM analysis

Figs. 12–14 are the morphology in the skin, sub-skin and core layer respectively, from which it can be seen obviously that there is a skin–core structure from surface to core in PA6/TPV system, especially, when the TPV content is higher, the gradient morphology is more obvious. For brevity, only the morphology of TPV2 is shown here. The skin–core structure is due to the shear stress field before the melt is solidified, which was first reported by Kato [42]. Then the skin–core structure in many blends was observed and thoroughly investigated [43,44]. Generally speaking, the deformed particles exist near the skin region and the spherical droplets often exist in the core. The viscosity ratio and the concentration of components as well as the addition of the compatibilizer might influence the hierarchy structure of the dispersed phase. In isotactic polypropylene (iPP)/EPR injection molded blends studied by Orazio et al. [45], with increasing EPR content the layered structure originally developed in the injection molded samples

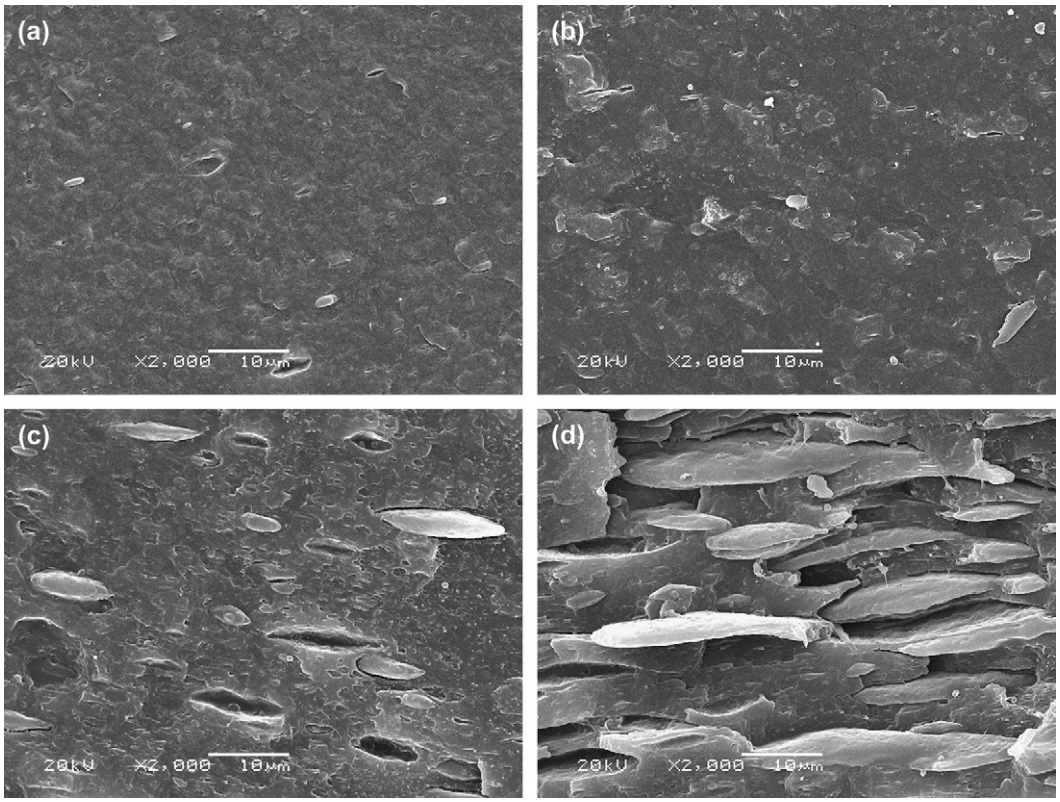

Fig. 12. SEM micrographs of the injection molded PA6/TPV2 samples in the skin. TPV2 content (by weight): (a) 5%, (b) 10%, (c) 20%, and (d) 30%.

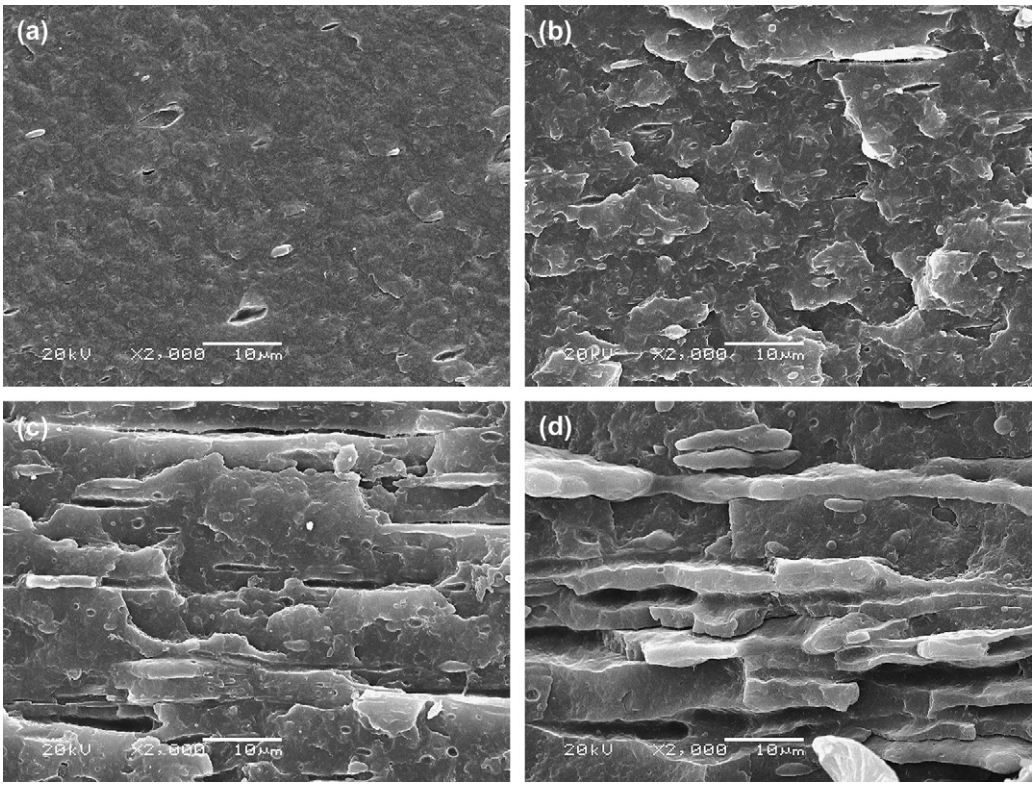

Fig. 13. SEM micrographs of the injection molded PA6/TPV2 samples in the sub-skin (the distance to surface is 500 μm). TPV2 content (by weight): (a) 5%, (b) 10%, (c) 20%, and (d) 30%.

of the iPP/EPR (80/20 by weight) blends was dramatically modified irrespective of the EPR microstructure. The morphology of injection molded high-density polyethylene (HDPE)/PA6 (25/75 by volume) blends, with or without compatibilizer, was investigated by Fellahi et al. [46,47]. A diminution of the thickness of the skin layer with interfacial modification was observed.

In our work, the dispersed TPV particles exhibit different shapes and sizes in the core, skin, and sub-skin layers. In the core layer, most TPV particles remain spherical in shape except a few slightly deformed ones, as shown in Fig. 14. In the skin and sub-skin layers, the dispersed phase TPV exhibits fine injection-induced TPV fibers, as shown in Figs. 12 and 13. From these micrographs, one can clearly observe that the average radial size increases and its distribution becomes wider with the increase of TPV content in each layer. The more TPV content, the more fibers are formed in skin and sub-skin layer, and the larger *L*/*D* (ratio of length to diameter) of the fibers. Because the coarsening rate of the phase structure in a certain blend increases with increasing concentration of the dispersed component, the diameter of spherical droplets in core layer increases with the increasing of TPV content [48].

4. Discussion

There are many mechanisms to explain the double yielding phenomenon so far. Mandelkern and co-workers [17,19] have postulated that the Flory and Yoon [49] mechanism of partial melting and recrystallization for the plastic deformation of semi-crystalline polymers can explain the origin of the double yielding phenomenon. Valerie and Seguela [50] proposed a slipping and shearing of crystal blocks mechanism based on Yamada and Takayanagi's hypothesis [51] that semi-crystalline polymers possess mosaic block structure of the crystalline lamellae. Brooks et al. thought that the first yield point was supposed to mark the onset of a non-linear viscoelastic behavior, namely a recoverable reorientation process of the lamellae within the spherulites, with little or no destruction of the lamellae themselves. The second yield point was supposed to be associated with the destruction of the lamellae lying at 45° to the stretch direction by c shear [15].

The mechanisms to explain the double yielding phenomenon of polymer blends [25–27] have also been put forward and detail information was mentioned in Section 1. However, these models developed for describing the yielding processes are difficult to be applied to our system. To the best of our knowledge, the deformation mechanisms for polymer blends should be strongly dependent on the phase morphology, as well as the interfacial interaction, the characteristic of the matrix and the dispersed phase. In this work, we mainly focus our attention on the effect of phase morphology caused by the introduction of TPVs.

From the stress–strain curves of double yielding phenomenon, it is deemed that the occurrence of the double yielding phenomenon must involves two or more kinds of microstructures corresponding to the two yield point which should satisfy the following conditions: (1) The microstructures must have

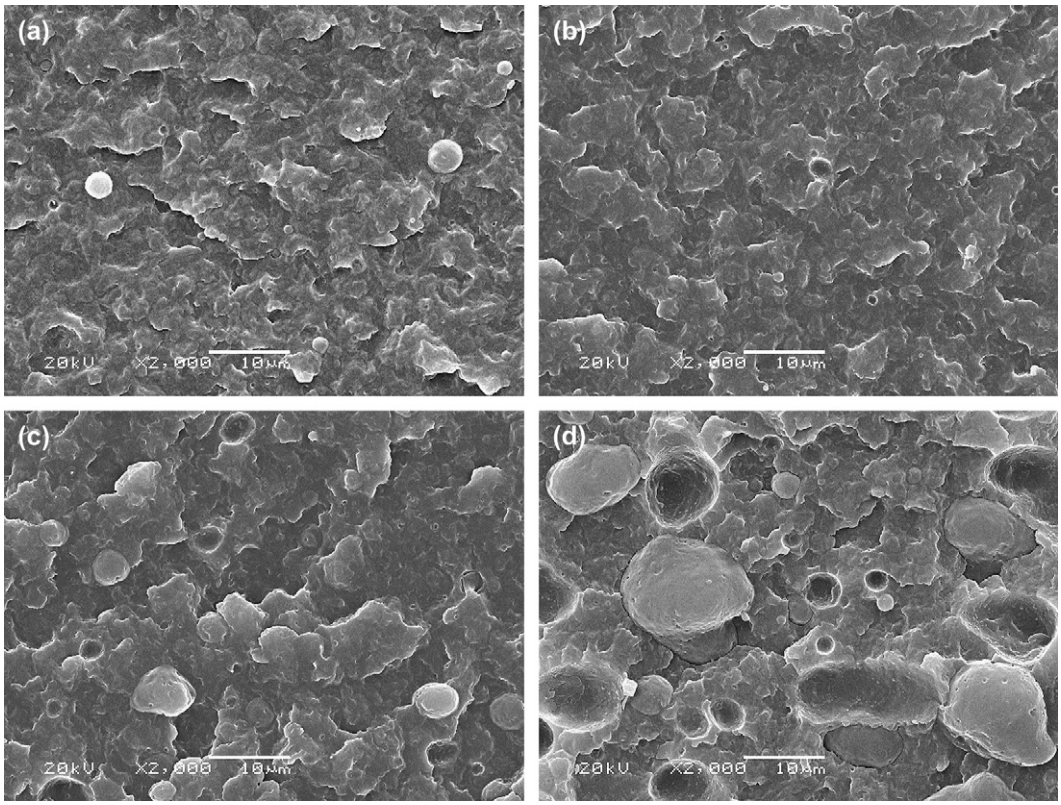

Fig. 14. SEM micrographs of the injection molded PA6/TPV2 samples in the core. TPV2 content (by weight): (a) 5%, (b) 10%, (c) 20%, and (d) 30%.

different response time during the tensile process, that is to say, the microstructure corresponding to the second yield point must have a delay time comparing with the first yield point during tension and its effect must be so significant that it can be exhibited in stress–strain curve, which is to make the two yield point separate. (2) The microstructure corresponding to the second yield point must supply force which should be so large that it can be exhibited in the stress–strain curve, which is to make the second yield point shift upperwards.

For our system, it can be seen that the dispersed phase exists in the form of fiber-like in the skin and sub-skin layer, while spherical droplets in the core layer from the SEM result. Fig. 15 is the schematic representation for the morphology of the injection molded PA6/TPV blend.

The development of the dispersed phase with different morphologies, that is, fiber and spherical droplet, is different during the tension and the stress state is different too. The schematic diagram of the morphology development and force analysis of the dispersed phase are shown in Fig. 16. When the tension was applied, the dispersed TPV was tightly embedded in the PA6 matrix. This led to a high compressive stress between the dispersed particles (TPV) and the matrix PA6 [52,53], which was represented by F_1. At the same time, a tensile force (F_2) was generated, which was the combination of two forces: (1) frictional force, resulting from a relative motion tendency existed at the interfaces, compressive force and a non-zero friction coefficient, all of which are the condition of the generation of frictional force [54]; (2) elongation stress, resulting from the separation between PA6 and TPV. There is interaction between PA6 and TPV in situ compatibilization TPV, the separation between PA6 and TPV during extension will generate a force along the direction of extension [11]. Because the fibers have larger specific surface area than that of the spherical droplets, there is larger interaction between PA6 and TPV, so the stress of matrix can be easier to transfer to the fibers than to the spherical droplets. Upon tension, the main deforming form of the fibers is elongation and the response time to elongation is short and the force F_2 is large. However, the main deforming form of spherical droplet is compression first, and then becomes elongation gradually with the deforming of spherical droplet and finally elongation becomes the main deforming form when the spherical droplets

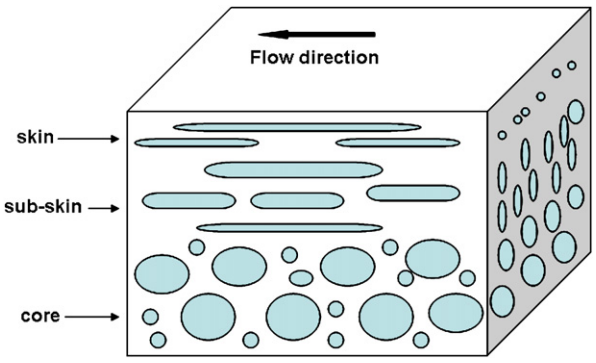

Fig. 15. The schematic representation for the morphology of the injection molded PA6/TPV blend.

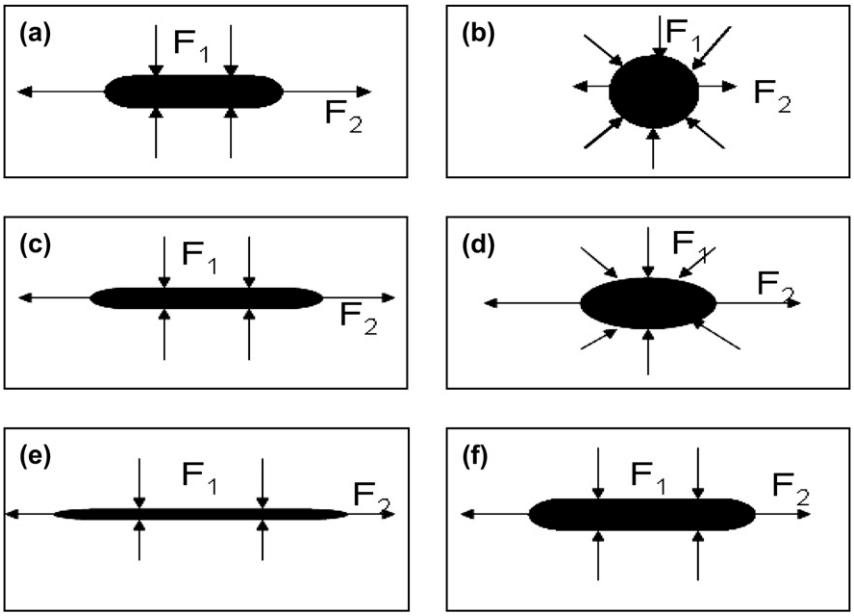

Fig. 16. The difference of the morphology development and force analysis of the dispersed phase particles during the elongation of the PA6/TPV blends. (a), (c) and (e) are the fiber; (b), (d) and (f) are the spherical droplet. (a) and (b) are the beginning of elongation; (c) and (d) are the first yield point; (e) and (f) are the second yield point. F_1 is the compressive force and F_2 is the elongation stress.

become fibers. In this process, the F_2 is so small that it can be omitted first, and then becomes larger gradually. The response time to elongation of dispersed phase in the core layer has a delay time with respect to those in the skin and sub-skin layer. When the delay time and F_2 of dispersed phase in the core layer are large enough, the double yielding phenomenon appears. So the first yield point occurs at the lower tensile strain might be caused by the deformation of the matrix and the dispersed phase in skin and sub-skin layer, while the second yield point may be correlated to deformation of the dispersed phase in core layer.

For the influencing factor studied in this paper, it could be seen that the experimental results accord well with the model described above.

First, the effect of TPV content. We know from the model that the first yield point is caused by the deformation of the matrix and the dispersed phase in the skin and sub-skin layer, the second yield point is correlated to deformation of the dispersed phase in the core layer and the strength of PA6 is bigger than TPV, while some PA6 is replaced by TPV with the increasing of TPV content in the skin, sub-skin and core layer, so the stress of the first yield point decreases. The stress of the second yield point decreases and the variation amplitude decreases because of the increasing of TPV content in the core layer, which can supply bigger force, and thus offset part of stress reduction. Because the fibers possess larger specific surface area than that of the spherical droplets, the stress of the matrix can be easier to transfer to the fibers and the fibers in skin and sub-skin layer almost deform with PA6 at the same time, and the strain of the first yield point does not change with the increasing of TPV content. The diameter of the TPV in core increases with the increasing of TPV content, which can be seen from SEM results, and thus the deformation time increases, so the strain of the second yield point increases.

Second, the effect of TPV characteristic. We know from the model that the first yield point and the second yield point both are correlated to the dispersed phase, so the characteristic of TPV has effect of the double yield phenomenon, and the higher the strength of TPV, the higher the stress of the first and the second yield point.

Third, the bigger the grafting degree, the higher the interfacial interaction between PA6 and TPV. In this system, the yield stress does not change with the increasing of the interaction between PA6 and dispersed phase while the stress transfer will become easier during elongation with the increasing of the interaction between PA6 and dispersed phase, and this lead to the advancement of the occurrence of the second yield point.

5. Conclusions

The double yielding phenomenon was observed in injection molded specimens of PA6/TPV blends. The effect of the dispersed phase content and the dispersed phase characteristic were studied. The results show that this phenomenon is in correlation with the dispersed phase content and characteristic. The stress at the first yield point decreased with the increasing dispersed phase content, with the strain being unvaried; the stress difference between the first and the second yield point decreased and the strain difference increased. The higher the strength of TPV, the higher the yield stress in both the first and the second yield point. The result of SEM shows that the morphology of injection molded PA6/TPV is a typical skin–core structure, which contributes to the double yielding

phenomenon. Considering all the results, a possible double yielding mechanism was proposed for the PA6/TPV blends.

Acknowledgements

The authors gratefully acknowledge the financial support of National Natural Science Foundation of China (Grant nos. 50503014, 50533050), the Opening Project of The Key Laboratory of Polymer Processing Engineering, Ministry of Education, China, the Special Funds for Major Basic Research (Grant no. 2005CB623808), and the Doctoral Research Foundation granted by the National Ministry of Education, China (Grant no. 20060610029).

References

[1] Zeng N, Bai SL, Sell CG, Hiver JM, Mai YW. Polym Int 2002;51:1439–47.
[2] Shonaike GO, Simon GP. Polymer alloys and blends. New York: Marcel Dekker; 1999.
[3] Utracki LA. Polymer blends handbook, vols. 1–2. Springer-Verlag; 2002.
[4] Patlazhan S, Schlatter G, Serra C, Boquey M, Muller R. Polymer 2006;47:6099–106.
[5] Chowdhury R, Banerji MS, Shivakumar K. J Appl Polym Sci 2007;104:372–7.
[6] Paul DR, Bucknall CB, editors. Polymer blends: formulation and performance. John Wiley & Sons; 2000.
[7] Heino M, Hietaoja P, Seppala J, Harmia T, Friedrich K. J Appl Polym Sci 1997;66:2209–20.
[8] Miles IS, Rostami S. Multicomponent polymer systems. Essex: Longman; 1993.
[9] Bai SL, Wang GT, Hiver JM, Sell CG. Polymer 2004;45:3063–71.
[10] Datta S, Lohse DJ. Polymeric compatibilizers: uses and benefits in polymer blends. Munich: Hanser; 1996.
[11] Baker WE, Scott CE, Hu GH. Reactive polymer blending. Hanser Gardner; 2001.
[12] Costa DA, Oliveira CM. J Appl Polym Sci 1998;69:857–64.
[13] Kolarik J. Polym Eng Sci 1996;20:2518–24.
[14] Gent AN, Madan S. J Polym Sci Part B Polym Phys 1989;27:1529–42.
[15] Brooks NW, Duckett RA, Ward IM. Polymer 1992;33:1872–80.
[16] Brooks NW, Unwin AP, Duckett RA. J Macromol Sci Phys 1995;34:29.
[17] Popli R, Mandelkern L. J Polym Sci Part B Polym Phys 1987;25:441–83.
[18] Muramatsu S, Lando JB. Polym Eng Sci 1995;35:1077–85.
[19] Lucas JC, Failla MD, Smith FL, Mandelkern L. Polym Eng Sci 1995;35:1117–23.
[20] Feijoo JL, Sanchez JJ, Muller AJ. J Mater Sci 1997;16:1721–4.
[21] Adhikari R, Buschnakowski M, Henning S. Double yielding in a styrene/butadiene star block copolymer. Macromol Rapid Commun 2004;25:653–8.
[22] Gaucher-Miri V, Seguela R. Macromolecules 1997;30:1158–67.
[23] Seguela R, Darras O. J Mater Sci 1994;29:5342–52.
[24] Spathis G, Kontou E. J Appl Polym Sci 2004;91:3519–27.
[25] Plaza AR, Ramos E, Manzur A, Olayo R, Escobar A. J Mater Sci 1997;32:549–54.
[26] Li ZM, Huang CC, Yang W, Yang MB, Huang R. Macromol Mater Eng 2004;289:1004–11.
[27] Jing B, Dai WD, Cao Q, Liu PS. Polym Bull 2006;57:359–67.
[28] Yang W, Shan GF, Wei SP, Li ZM, Xie BH, Yuan XH, et al. China Plast 2005;19:22–6.
[29] Shan GF, Yang W, Xie BH, Li ZM, Feng JM, Yang MB. Polym Test 2005;24:704–11.
[30] Shan GF, Yang W, Xie BH, Li ZM, Feng JM, Yang MB. Polym Test 2006;25:452–9.
[31] Shan GF, Yang W, Tang XG, Yang MB, Xie BH, Fu Q. J Polym Sci Part B Polym Phys 2007;45:1217–25.
[32] Shan GF, Yang W, Yang MB, Xie BH, Fu Q. Polymer 2007;48:2958–68.
[33] Hoashi K, Kawasaki N, Andrews RD. In: Lenz RW, Stein RS, editors. Structure and properties of polymer films. New York: Plenum Press; 1973. p. 283.
[34] Fisher WK. US Patent 3,758,643; 1973.
[35] Fisher WK. US Patent 3,862,106; 1975.
[36] Shariatpanahi H, Nazokdast H, Dabir B, Sadaghiani K. J Appl Polym Sci 2002;86:3148–59.
[37] Coran AY, Patel R. Rubber Chem Technol 1981;54:892–903.
[38] Zhang YC, Chen JY, Li HL. Polymer 2006;47:4750–9.
[39] Xantos M. Polym Eng Sci 1988;28:1392–400.
[40] Goharpey F, Nazochdast H, Katbab AA. Polym Eng Sci 2005;1:84–94.
[41] Edwin AM, Betty LL. Macromol Symp 2006;242:131–9.
[42] Kato K. Polymer 1968;9:225.
[43] Bureau MN, Kadi HE, Denault J, Dickson JI. Polym Eng Sci 1997;37:377–90.
[44] Taha M, Frerejean V. J Appl Polym Sci 1996;61:969–79.
[45] Orazio LD, Mancarella C, Martuscelli E, Cecchin G, Corrieri R. Polymer 1999;40:2745–57.
[46] Fellahi S, Fisa B, Favis BD. ANTEC Tech Pap 1993;39:211.
[47] Fellahi S, Favis BD, Fisa B. Polymer 1996;37:2615–26.
[48] Fortelny I, Zivny A, Juza J. J Polym Sci Part B Polym Phys 1999;37:181–7.
[49] Flory PJ, Yoon DY. Nature 1978;272:226–9.
[50] Valerie GM, Seguela R. Macromolecules 1997;30:1158–67.
[51] Yamada K, Takayanagi M. J Appl Polym Sci 1979;24:781.
[52] Kurauchi T, Ohta T. J Mater Sci 1984;19:1699.
[53] Koo KK, Inoue T, Miyasaka K. Polym Eng Sci 1985;25:741.
[54] Li ZM, Fu XR, Yang SY, Yang MB, Yang W, Huang R. Polym Eng Sci 2004;44:1561.